

Intrinsic Geometry of the Stock Market from Graph Ricci Flow

Bhargavi Srinivasan

CNRS, Laboratoire de Physique Théorique et Modèles Statistiques, Université Paris-Saclay, 91405 Orsay, France

(Dated: October 21, 2025)

We use the discrete Ollivier-Ricci graph curvature with Ricci flow to examine the intrinsic geometry of financial markets through the empirical correlation graph of the NASDAQ 100 index. Our main result is the development of a technique to perform surgery on the neckpinch singularities that form during the Ricci flow of the empirical graph, using the behavior and the lower bound of curvature of the fully connected graph as a starting point. We construct an algorithm that uses the curvature generated by intrinsic geometric flow of the graph to detect hidden hierarchies, community behavior, and clustering in financial markets despite the underlying challenges posed by a highly connected geometry.

The study of the economy as a complex dynamical system has been the focus of a great deal of attention over the past two and a half decades in the field of econophysics[1]. Stock correlations have emerged to become a crucial quantity in the study of stock markets.

The empirical correlation matrix C_{ij} based on the time series of returns r_i for stock i is computed from the Pearson correlation coefficients by the usual definition with mean \bar{r}_i and variance σ_i : $C_{ij} = \frac{\langle (r_i - \bar{r}_i)(r_j - \bar{r}_j) \rangle}{\sigma_i \sigma_j}$

We can then associate a distance that defines an edge weight given by $w_{ij} = \sqrt{2(1 - C_{ij})}$ which is our fully connected graph, with all positive weights.

A remarkable property of stock returns is their positive correlation which leads to the emergence of a market index[2]. The spectral properties of the stock correlation matrix have been extensively analyzed and constitute an insightful tool in the risk management of stock portfolios.

On the other hand, the correlation matrix can be used to construct a network with the nodes given by the stocks, which provides a weighted, undirected, fully connected graph.

Existing techniques seek to reduce the connectivity of the graph, by pruning links, to make it more amenable to study. For instance, most standard techniques rely on the minimal spanning tree (MST) to reduce the connectivity of the network[3],[4]. Pruning links to create an MST changes the topology and geometry of the network. In addition, the edge weights of the correlation matrix are very closely spaced, which poses a challenge for MST methods, since their outcome is sensitive to slight differences in the edge weights. Other clustering techniques make assumptions about the geometry of the system or the number of clusters involved (k-means, spectral clustering)[5],[6],[7].

It would be attractive to use recent advances from graph theory, which could shed light on the geometric structure of this network using the full connectivity information without further assumptions. Recent developments in graph theory originating from the adaptation of differential geometry techniques to discrete graphs have shown great potential [8],[9],[10],[11],[12],[13],[14]. The Ricci flow[15], used with great success to solve the

Poincaré conjecture[16],[17],[18], is an intrinsic flow of the Ricci curvature tensor, which, coupled with surgery, can be used to decompose a manifold into a connected sum of simpler manifolds. Given the dense connectivity and close distribution of the edge weights of our network, techniques of intrinsic geometric flow provide an attractive alternative to reveal the hidden hierarchy of the data without imposing an external structure.

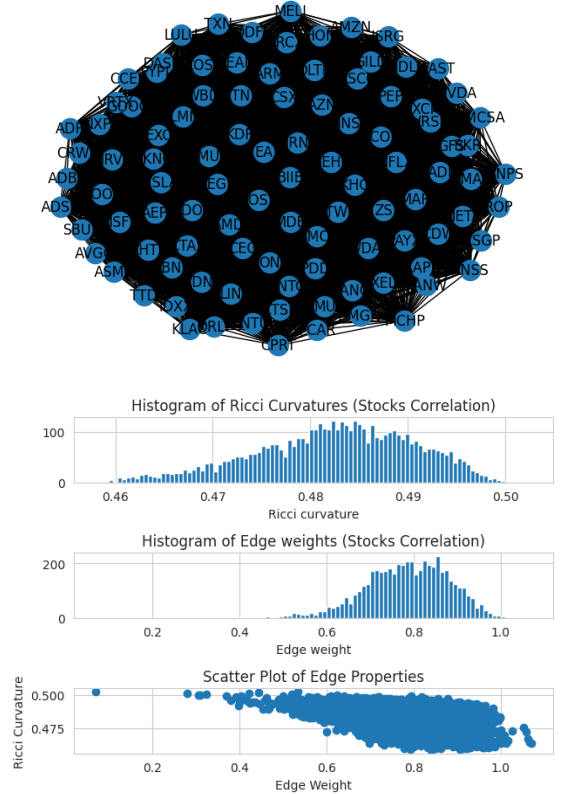


FIG. 1. NASDAQ-100 complete graph

Edge-centric approaches involving graph curvature are increasingly emerging as the method of choice to analyze complex graphs. Combinatorial Forman-Ricci[19],[14],[20] curvature and probabilistic Ollivier-

Ricci curvature[8],[9],[10] (ORC) are key developments that have permitted the adaptation of differential geometry methods to discrete structures such as graphs. The correlation matrix, being a fully connected graph, already provides an important indicator of the geometry of the system. Graph curvature has been evoked in the context of the stock market but in these works the network was again replaced by the MST[21],[22],[23],[24]. In this letter, we use the Ollivier-Ricci curvature to construct and analyze the weighted network generated by the stock market as a weighted complete graph. Our main result is to propose a discrete Ricci flow algorithm with surgery based on curvature along neckpinch singularities which allows us to analyze the structure and intrinsic geometry of fully connected graphs with positive curvature, such as the stock market. Detailed comparisons with state-of-the-art techniques such as MST and PCA are the subject of a longer paper[25].

Hamilton's Ricci flow deforms the metric in a fashion analogous to the heat equation,

$$\frac{\partial g_{\mu\nu}}{\partial t} = -2R_{\mu\nu} \quad (1)$$

where $g_{\mu\nu}$ is the metric tensor and $R_{\mu\nu}$ the Ricci curvature tensor. This second-order non-linear PDE smooths out irregularities in the metric but leads to singularities that can be removed by a procedure known as surgery. There are two steps in adapting Ricci flow to graphs. A breakthrough in adapting this technique to discrete systems came from the definition of coarse curvature or Ollivier-Ricci curvature (ORC) from the work of Ollivier[8],[9],[10]. The second step is devising the flow, as described below.

The Ollivier-Ricci curvature is based on the optimal transport of probability measures associated with a lazy random walk. The discrete Ollivier-Ricci curvature κ_{ij} on graph edge $ij \in E$, for a graph $G = (V, E, w)$ with vertices V , edges E and weights w , compares the Wasserstein distance between two nodes with the shortest distance or edge weight through

$$\kappa_{ij} = 1 - \frac{W(m_i, m_j)}{d(i, j)} \quad (2)$$

where $d(i, j)$ is the shortest distance between nodes i and j . The Wasserstein distance is defined in the appendix and is related to the probability measures on each site. As explained in the appendix, we use a lazy random walk probability measure, with idleness parameter $\alpha = 1/2$. Therefore, we drop the α index, with the understanding that $\alpha = 1/2$ in this work.

From this definition, we see that if the nodes i and j belong to the same community, they tend to share neighbors. Therefore the cost of transporting mass is smaller and the Wasserstein distance is no greater than $d(i, j)$. Thus intra-community edges have a positive Ollivier-Ricci curvature. On the other hand, if nodes i and j

are from different communities, they tend to have fewer neighbors in common. Therefore, transporting mass from i to j necessarily involves passing through the edge ij and the Wasserstein distance is larger than $d(i, j)$. Therefore the curvature of edge ij is negative and the link is hyperbolic. On a flat graph, the Wasserstein and $d(i, j)$ distances are identical and the curvature is zero. If all the links in a graph have zero curvature, then the graph is called Ricci-flat. The regular grid is an example of a Ricci-flat graph.

With this definition of coarse curvature, we can now build the Ricci flow, to generate a time-dependent family of weighted graphs $G(V, E, w(t))$, such that the weight $w_{ij}(t)$ on edge ij changes proportionally to the Ollivier-Ricci curvature $\kappa_{ij}(t)$ at time t . Ollivier[9],[10] suggested a flow with continuous time t ,

$$\frac{d}{dt}w_e(t) = -\kappa_e(t)w_e(t) \quad (3)$$

where edge $e \in E$, with Ollivier-Ricci curvature κ_e and edge weight $w_e(t)$. Jost and co-workers used a discrete time algorithm with the Forman-Ricci curvature. Sia and co-workers[26] introduced an algorithm based on surgery with curvature but links were not updated. Ni and co-workers[27] suggested a discrete-time algorithm while updating the edge-weights. Each iteration of this algorithm consists in updating all edge weights of the network simultaneously. The l^{th} step of this process gives

$$w_{ij}^{(l+1)} = (1 - \kappa_{ij}^{(l)})d^{(l)}(i, j) \quad (4)$$

where $w_{ij}^{(l)}$ is the weight of edge ij at the l^{th} iteration, $\kappa_{ij}^{(l)}$ is the Ricci curvature of edge ij at the l^{th} iteration, and $d^{(l)}(i, j)$ is the shortest path distance induced by the weights $w_{ij}^{(l)}$. Initially $w_{ij}^{(0)} = w_{ij}$ and $d^{(0)}(i, j) = d(i, j)$, the initial weights and distances of the graph. Therefore at the l^{th} iteration, the edge weights are replaced by the Wasserstein distance to define the graph at the $(l + 1)^{th}$ iteration. The procedure is then repeated to obtain the new Ricci curvature. The Ricci flow has the effect of bringing the positive edges closer and pushing the negatively curved edges further apart. This effect is used to perform surgery on the network and separate the network into communities.

With this definition of the Ricci curvature, propagating these values by the Ricci flow tends to exaggerate the differences between the different types of links. Links with positive curvature tend to cluster together and links of negative curvature tend to move further and further apart under the Ricci flow, while flat links are unaffected. While community detection in graphs is a very active field of research[28],[29],[30], this brings a new approach to cluster complex networks[20],[27]. The multiscale structure of networks has been studied using dynamical ORC[31].

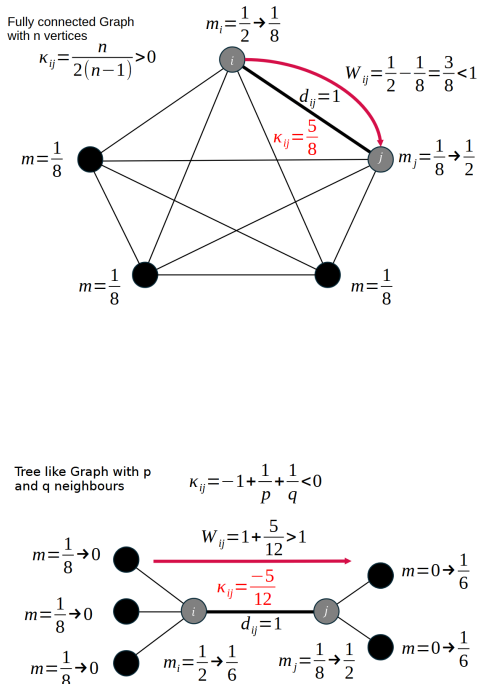


FIG. 2. Illustration of Wasserstein distance and Graph curvature on fully connected and tree-like graphs

How do we look for hierarchies in such a network? In our work, we consider as our starting point the fully-connected graph with equal weights. In the literature, the fully connected graph with equal edge weights is often referred to as the discrete equivalent of the spherical manifold. Therefore, the expectation of communities bound together and separated by well-traveled or hyperbolic links does not hold here. The eigenvalues of the Laplacian of the complete graph are known to be 0 and $\frac{n}{n-1}$ with multiplicity $n-1$. If we consider the complete graph with N nodes and $\alpha = 1/2$ the Wasserstein calculation is illustrated in Fig. (2) for a 5 node graph. We see that $W_{ij} \leq 1$ therefore, the Ricci curvature is always positive. So for a fully connected graph with N nodes and all equal edge weights, the Ricci curvatures of all edges are equal and given by $\kappa_{ij} = (1 - \alpha) \frac{n}{n-1} = \kappa$. It is known[12] that the Lin-Lu-Yau-Ricci curvature $\lim_{\alpha \rightarrow 1} \frac{\kappa_{ij}}{(1-\alpha)} = \frac{n}{n-1}$ of the complete graph K_n is the only graph with a constant curvature greater than 1, which fits with the value above for $\alpha = 1/2$. The eigenvalues of the Laplacian of the complete graph are the same as the Lin-Lu-Yau-Ricci curvatures. In the case of the NASDAQ 100 network, if we approximated equal edges, with $\alpha = 1/2$, we would have $\kappa = 0.505$. Thus, this complete

graph is a highly degenerate graph. It is expected that when the edge weights are not all equal, this degeneracy will be broken.

In Fig. 1 we present our construction of the NASDAQ-100 graph with empirical edge weights, constructed from real-life data. We recovered the values of stock prices from Yahoo! Finance[32] using the components of the NASDAQ-100 Index from [33]. We calculate the returns and average over a period of five years from 1/1/2020-20/11/2024. Based on the edge weights, we obtain a histogram of Ricci curvatures[27],[34]. The histogram is shifted downward from the complete graph at 0.505, though being all positive retain the spherical aspect of this graph. This is reflected in the downward shift of the distances from 1. However, the curvatures are very closely distributed around the median, and a priori, this is not a very favorable situation to select a given link for surgery. The correlation of this graph is 38%, which means that there is an average edge-weight of 0.78. In Fig. 1 we can see the distributions of the edge weights and they are shifted downwards from 1 and are all very tightly distributed around a median value of 0.8, in accordance with the correlation. Here the κ_{ij} are all positive which corresponds to a graph of positive curvature, while the edge weights are not identical in a fully connected graph, due to the connectivity. With the Ricci coarse curvature, we are able to use the full correlation matrix to build a network and carry our Ricci flow without any assumptions about the number of clusters.

The geometry of three and four manifolds under Ricci flow was studied extensively by Hamilton. A limited version of the Poincaré theorem for Riemannian manifolds of strictly positive curvature was proved by Hamilton[15]. In the case of manifolds with positive curvature, it is known that evolution under Ricci flow leads to neck-pinch singularities which are removed by surgery[35]. A dumbbell-like manifold under Ricci flow develops a neck-pinch singularity and surgery is carried out along the cylindrical link[36].

First, let us consider the case of a Ricci flow on the fully connected graph with equal edge weights. It is clear that if we look at the graph with equal weights, if we do not update edge weights using the algorithm, the Wasserstein distance and Ricci curvature are unchanged. If we update the edge weight, Ricci flowing the graph will lead to shortening the edge weights and eventually to a singularity. Yet, the graph remains self-similar, in the sense that it is a fully connected graph with equal edge weights, which decrease with time, eventually leading to a point-like singularity. All edges remain equal, and there is no question of separating this graph into communities through different edges. Other approaches exist in the literature where the normalized Ricci flow is used, in which case there is no singularity, though self-similarity remains.

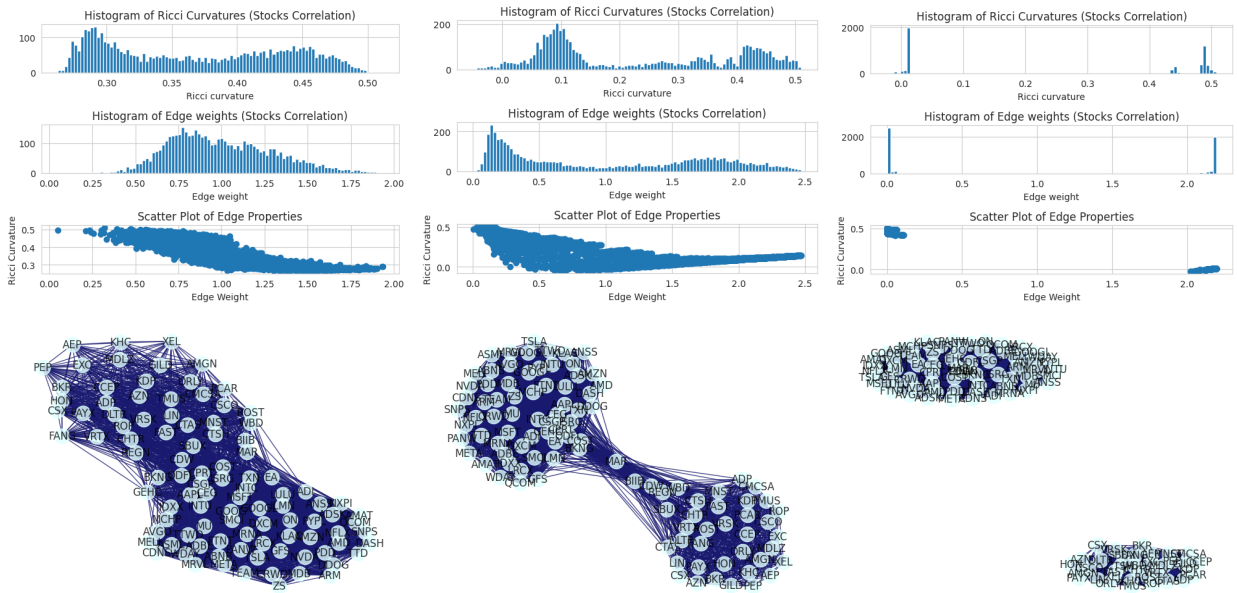


FIG. 3. NASDAQ-100 Ricci flow after 5, 10 and 20 iterations with surgery on the 20th iteration

The situation is entirely different when we consider the fully connected NASDAQ-100 graph with distinct empirical edge weights obtained from the stock market. The challenge here is to analyze the empirical NASDAQ graph to highlight features and communities. In the continuum the neckpinch singularities are identified, and surgery is performed to separate the original manifold into a connected sum of manifolds while avoiding collapse. In the discrete context, the key step is to be able to identify the neckpinch singularities. Here we will attempt a similar decomposition of our graph with the expectation that we will find spherical ‘communities’. These are not connected by hyperbolic links, therefore the challenge is to isolate them. One way to do this would be the development of a locally flat neckpinch singularity, which can be embedded into a locally flat manifold.

We expect that Ricci flow should shrink the edges of a community to regions of large positive curvature. This is indeed the case. If we use edge weights as a measure, it is still not clear how to carry out surgery in the fully connected manifold using distances. In [26] edge curvature alone without Ricci flow was used, with the argument that triangles are a good index of community formation. We suggest in this work, based on Ricci flow and the intuition obtained from the fully connected graph, that curvature is a good metric to use.

We carried out the Ricci flow on the NASDAQ graph with $\alpha = \frac{1}{2}$ and a discrete time step[34]. In Fig. (3) we see that after just 5 iterations of Ricci flow, the distribution of edge weights begins to flatten out. The distri-

bution of curvatures is more remarkable; we begin to see the data split into two peaks. This confirms our intuition that edge curvature is a sensitive measure of clustering in data. We expect that a neckpinch singularity develops.

From Fig. (3), we notice that after just 5 iterations of Ricci flow, the histogram of edge weights has become much wider. The curvature histogram is even more pronounced, with the appearance of two peaks. We make a scatter plot of edge weight vs. curvature, and this is widely dispersed. Visually we see that fully connected network has already started separating into two communities. After 10 iterations, these features are much more pronounced, with the appearance of a dumbbell-shape and a neckpinch between the two communities. From the spread of the scatter plot, it is not yet clear how to perform surgery. By 20 iterations, the histograms of edge weight and edge curvature are completely changed. The system is split into two communities. The scatter plot provides us with the means to select the links for surgery. We perform surgery along the zero-curvature links, which correspond to the long flat links that separate the two communities.

After 20 iterations, we see a clear separation between different clusters. This is better seen in a scatter plot. We plot the edge weight and curvature scatter plot. We find the links flattening and the curvature approaches zero.

From Lin and Yau[13],[37], the infinite weighted graph has a lower bound to the ORC given by $\kappa_{ij} \geq \kappa_{ij,min} = \frac{2}{d_i} + \frac{2}{d_j} - 2$, where d_i is the degree of link i . The lower bound has been further developed for hypergraphs[38].

In the limit of the infinite complete graph with equal edge weights, this gives a value for $\kappa_{ij,min} = \frac{2(3-n)}{(n-1)}$. For the NASDAQ-100 graph this gives $\kappa_{ij,min} \approx -1.96$. Naively, this would correspond to a length of $d_{ij} \approx 2.96$ as the longest edge length possible. We find after 20 iterations that the graph splits into two communities, with very short edge weights and positive curvature. These two communities are separated by long, flat links with curvature zero and edge weights around 3. It is interesting to note that the fully connected graph which satisfies strict positivity of the curvature before the Ricci flow, still obeys the lower bound condition, even with unequal edge weights. This brings us to the question of surgery in such a graph, it would seem appropriate to use the flattening that develops along the neck pinch singularity to perform surgery along the zero-curvature links. This suggests that the geometry of the NASDAQ-100 graph is a prominent influence on its properties. The reason is that the degree of the graph seems to play a key role in influencing the lower bound, even without equal edge weights.

With this procedure for surgery, based on curvature, we can analyze the system through several levels of Ricci flow followed by surgery. In this work, we sketch the clustering obtained by our technique, with a more detailed financial analysis of the clusters presented in another work[39]. The NASDAQ-100 is a tech-heavy index. After the first level of Ricci flow, followed by surgery using the method described above, the cluster splits into two communities of 66 and 35 stocks. The larger cluster is clearly tech-driven and we first focus on this. The second level of Ricci flow leads to a basket of 16 semiconductor stocks. It is encouraging to see that Ricci flow can identify the semiconductor stocks. However Nvidia is absent from this cluster. The level 3 Ricci flow of the 50 stock cluster leads to the separation of a cluster of 10 stocks. When we examine these stocks, it is clear that they are outliers. Moderna, which was a very poor performer was subsequently dropped from the NASDAQ in December 2024. Analyzing the 40 stock cluster leads to the separation of biotech stocks and Supermicro stock. The cluster of the remaining 35 stocks splits into two roughly equal groups of 17 and 18 stocks. We name the 17 stock cluster 'Big Tech' which contains Nvidia and Amazon amongst others, so Nvidia finds its position in the market makers stock over the more limited semiconductor stocks. Tesla is in the other cluster.

The other level 1 cluster of 35 stocks seems to contain non-cyclicals, which we are then able to cluster into Healthcare staples, Energy staples and Industrials. See Fig. (4). The detailed cluster components are listed in the tables in the appendix.

A detailed analysis of the clusters from the point of view of econophysics is underway[39]. We are carrying out more systematic comparisons with MST and varia-

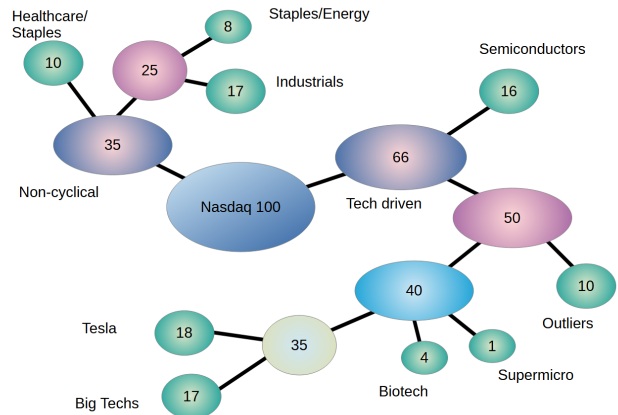


FIG. 4. Level 5 clustering of NASDAQ-100

tions of α , which will be presented in a longer paper[25]. It is also important to delve deeper into the clusters provided by this method and to study a larger, less tech-heavy index such as the S&P500 index. The behavior around crashes is also being investigated. .

In conclusion, we study the NASDAQ-100 stock index from the point of view of a fully connected network and provide an algorithm to carry out surgery based on curvature values after Ricci flow on this graph. We are able to develop a novel clustering technique on this fully connected graph, without assumptions about the number of clusters. We are able to identify outliers. Our curvature based approach provides an attractive alternative to MST to study the geometric properties of the stock market. Our technique provides a novel, curvature based criterion to perform surgery on highly-connected graphs with initial positive curvature.

We wish to acknowledge the support of the CNRS and LPTMS.

-
- [1] J.-P. Bouchaud and M. Potters, *Theory of Financial Risk* (Alea-Saclay, Eyrolles, Paris, 1997).
- [2] L. Laloux, P. Cizeau, J.-P. Bouchaud, and M. Potters, Noise dressing of financial correlation matrices, *Physical Review Letters* **83**, 1467–1470 (1999).
- [3] M. Tumminello, F. F. Lillo, and R. N. Mantegna, Hierarchically nested factor model from multivariate data, *EPL (Europhysics Letters)* **78**, 30006 (2007).
- [4] G. Marti, F. Nielsen, M. Bińkowski, and P. Donnat, A review of two decades of correlations, hierarchies, networks and clustering in financial markets, in *Progress in Information Geometry* (Springer International Publishing, 2021) p. 245–274.
- [5] S. Lloyd, Least squares quantization in pcm, *IEEE transactions on information theory* **28**, 129 (1982).
- [6] J. MacQueen, Multivariate observations, in *Proceedings of the 5th Berkeley Symposium on Mathematical Statistics and Probability*, Vol. 1 (1967) pp. 281–297.
- [7] F. R. K. Chung, *Spectral Graph Theory*, Vol. 92 (American Mathematical Society, Providence, RI, 1997).
- [8] Y. Ollivier, Ricci curvature of metric spaces, *C. R. Acad. Sci. Paris, Ser. I* **345**, 643 (2007).
- [9] Y. Ollivier, Ricci curvature of markov chains on metric spaces, *J. Funct. Anal.* **256**, 810 (2009).
- [10] Y. Ollivier, Probabilistic approach to geometry (Math. Soc. of Japan, Tokyo, Japan, 2010) Chap. A survey of ricci curvature for metric spaces and markov chains, pp. 343–381, <https://doi.org/10.2969/aspm/05710343>.
- [11] J. Lott and C. Villani, Ricci curvature for metric-measure spaces via optimal transport, *Annals Maths. Second Ser.* **169**, 903 (2009).
- [12] Y. Lin, L. Lu, and S.-T. Yau, Ricci curvature of graphs, *Tohoku Math. J.* **63**, 605 (2011).
- [13] Y. Lin and S.-T. Yau, Ricci curvature and eigenvalue estimate on locally finite graphs, *Math. Res. Lett.* **17**, 343 (2010).
- [14] R. P. Sreejith, K. Mohanraj, J. Jost, E. Saucan, and A. Samal, Forman curvature for complex networks, *J. Stat. Mech. Theory Exp.* **2016**, 063206 (2016).
- [15] R. S. Hamilton, Three-manifolds with positive ricci curvature, *Journal of Differential Geometry* **17**, 255 (1982).
- [16] G. Perelman, The entropy formula for the ricci flow and its geometric applications, <https://arxiv.org/abs/math/0211159> (2002).
- [17] G. Perelman, Ricci flow with surgery on three-manifolds, <https://arxiv.org/abs/math/0303109> (2003).
- [18] G. Perelman, Finite extinction time for the solutions to the ricci flow on certain three-manifolds, <https://arxiv.org/abs/math/0307245> (2003).
- [19] R. Forman, Bochner’s method for cell complexes and combinatorial ricci curvature, *Discrete Comput Geom* **29**, 323 (2003).
- [20] M. Weber, E. Saucan, and J. Jost, Characterizing complex networks with Forman-Ricci curvature and associated geometric flows, *J Complex Netw* **5**, 527 (2017).
- [21] R. S. Sandhu, T. T. Georgiou, and A. T. Tannenbaum, Ricci curvature: An economic indicator for market fragility and systemic risk, *Science Advances* **2** (2016), DOI: 10.1126/sciadv.1501495.
- [22] A. Samal, H. K. Pharasi, S. J. Ramaia, H. Kannan, E. Saucan, J. Jost, and A. Chakraborti, Network geometry and market instability, *R. Soc. Open Sci.* **8**, 201734 (2021).
- [23] M. Keller-Ressel and S. Nargang, The hyperbolic geometry of financial networks, *Sci Rep* **11**, 4732 (2021), DOI:10.1038/s41598-021-83328-4.
- [24] P. van der Hoorn, W. J. Cunningham, G. Lippner, C. Trugenberger, and D. Krioukov, Ollivier-ricci curvature convergence in random geometric graphs, *Phys. Rev. Res.* **3**, 013211 (2021).
- [25] B. Srinivasan, Comparison of clustering of complete graphs from ricci flow and mst, in preparation (2025).
- [26] J. Sia, E. Jonckheere, and P. Bogdan, Ollivier-ricci curvature-based method to community detection in complex networks, *Scientific reports* **9**, 9800 (2019), DOI: 10.1038/s41598-019-46079-x.
- [27] C.-C. Ni, Y.-Y. Lin, F. Luo, and J. Gao, Community detection on networks with ricci flow, *Scientific reports* **9**, 1 (2019).
- [28] S. Fortunato, Community detection in graphs, *Phys. Rep.* **486**, 75 (2010).
- [29] M. Girvan and M. E. J. Newman, Community structure in social and biological networks, *Proc. Natl. Acad. Sci. USA* **99**, 7821 (2002).
- [30] M. E. J. Newman and M. Girvan, Finding and evaluating community structure in networks, *Phys. Rev. E* **69**, 026113 (2004).
- [31] A. Gosztolai and A. Arnaudon, Unfolding the multiscale structure of networks with dynamical ollivier-ricci curvature, *Nature Communications* **12**, 4561 (2021).
- [32] Yahoo finance database, <https://finance.yahoo.com/>, accessed on 20th November, 2024.
- [33] Wikipedia, NASDAQ 100, <https://en.wikipedia.org/wiki/Nasdaq-100>, accessed on 20th November, 2024.
- [34] C.-C. Ni, Y.-Y. Lin, F. Luo, and J. Gao, <https://github.com/saibalmars/GraphRicciCurvature>.
- [35] R. S. Hamilton, The formation of singularities in the ricci flow, *Surveys in Differential Geometry* **2**, 7 (1982).
- [36] S. Angenent and D. Knopf, An example of neckpinching for ricci flow on s^{n+1} , *Math. Res. Lett.* **11**, 493 (2004).
- [37] J. Jost and S. Liu, Ollivier’s ricci curvature, local clustering and curvature-dimension inequalities on graphs, *Discrete Comput Geom* **51**, 300 (2014).
- [38] W. Kang and H. Park, Accelerated evaluation of ollivier-ricci curvature lower bounds: Bridging theory and computation, *arXiv preprint arXiv:2405.13302* (2024).
- [39] B. Srinivasan, Clustering the nasdaq-100 through ricci flow, in preparation (2025).

Ticker	Name	Sector	Sub-Industry
KLAC	KLA Corporation	IT	Semiconductors Equip
ADI	Analog Devices	IT	Semiconductors
LRCX	Lam Research	IT	Semiconductors Equip
AMAT	Applied Materials	IT	Semiconductors Equip
MCHP	Microchip Technology	IT	Semiconductors
ARM	ARM Holding	IT	Semiconductors
ASML	ASML Holdings	IT	Semiconductors Equip
AVGO	Broadcom	IT	Semiconductors
MRVL	Marvell Technology	IT	Semiconductors
MU	Micron Technology	IT	Semiconductors
NXPI	NXP Semiconductors	IT	Semiconductors
ON	Onsemi	IT	Semiconductors
QCOM	Qualcomm	IT	Semiconductors
GFS	GlobalFoundries	IT	Semiconductors
TXN	Texas Instrument	IT	Semiconductors
INTC	Intel	IT	Semiconductors

TABLE I. Level2 Cluster: Semiconductor Industry

Ticker	Name	Sector	Sub-Industry
ABNB	Airbnb	Cons Disc	Hotel, resort Cruise
MRNA	Moderna	Health Care	Biotech
PDD	PDD Holding	Cons Disc	Broadline retail
TEAM	Atlassian	IT	Appli software
CRWD	CrowdStrike	IT	System software
TTD	Trade Desk	Comm Servic	Advert
DASH	DoorDash	Cons Disc	Specialized cons services
DDOG	Datadog	IT	Appli software
ZS	Zscaler	IT	Appli software
MDB	MongoDB	IT	System software

TABLE II. Level3 Cluster: Outlier

Ticker	Name	Sector	Sub-Industry
GEHC	GE HealthCare	Health Care	Health Care Equip
CEG	Constellation Energy	Utilities	Electric Utilities
REGN	Regeneron Pharmaceuticals	Health Care	Biotechnology
BIIB	Biogen	Health Care	Biotechnology

TABLE III. Level4 Cluster: Biotech

Ticker	Name	Sector	Sub-Industry
SMCI	Supermicro	IT	Tech Hardware, Storage & Peripherals

TABLE IV. Level4 Cluster: SuperMicro

Ticker	Name	Sector	Sub-Industry
AAPL	Apple Inc.	IT	Tech Hardw, Stora, Periph
ADBE	Adobe Inc.	IT	Application Software
TTWO	Take-Two Inter	Comm Serv	Home Entertainment
AMD	Advanced Micro Dev	IT	Semiconductors
AMZN	Amazon	Cons Disc	Broadline Retail
ANSS	Ansys	IT	Application Software
CDNS	Cadence Design Sys	IT	Application Software
COST	Costco	Cons Staples	Merch Retail
EA	Electronic Arts	Comm Serv	Home Entertainment
GOOGL	Alphabet (A)	Comm Serv	Media & Services
GOOG	Alphabet (C)	Comm Serv	Media & Services
INTU	Intuit	IT	Application Software
META	Meta Platforms	Comm Serv	Media & Services
MSFT	Microsoft	IT	Systems Software
NFLX	Netflix	Comm Serv	Movies & Entertainment
NVDA	Nvidia	IT	Semiconductors
SNPS	Synopsys	IT	Application Software

TABLE V. Level5 Cluster: Big Techs

Ticker	Name	Sector	Sub-Industry
TSLA	Tesla, Inc.	Cons Disc	Auto Manufacturers
ADSK	Autodesk	IT	Application Software
WDAY	Workday, Inc.	IT	Application Software
BKNG	Booking Holdings Inc.	Cons Disc	Hotels, Resorts, Cruise Lines
CDW	CDW Corporation	IT	Tech Distributors
CPRT	Copart	Industrials	Diversified Support Serv
CSGP	CoStar Group	Real Estate	Real Estate Serv
DXCM	DexCom	Health Care	Health Care Equip
FTNT	Fortinet	IT	Systems Software
IDXX	Idexx Laboratories	Health Care	Health Care Equip
ILMN	Illumina, Inc.	Health Care	Life Sciences Tools & Serv
ISRG	Intuitive Surgical	Health Care	Health Care Equip
LULU	Lululemon Athletica	Cons Disc	Apparel, Accessories
MAR	Marriott International	Cons Disc	Hotels, Resorts, Cruise Lines
MELI	MercadoLibre	Cons Disc	Broadline Retail
ODFL	Old Dominion Freight Line	Industrials	Cargo Ground Transp
PANW	Palo Alto Networks	IT	Systems Software
PYPL	PayPal	Financials	Transaction & Payment Serv

TABLE VI. Level5 Cluster: Tesla group

Ticker	Name	Sector	Sub-Industry
VRTX	Vertex Pharmaceuticals	Health Care	Biotechnology
AEP	American Electric Power	Utilities	Electric Utilities
AMGN	Amgen	Health Care	Biotechnology
AZN	AstraZeneca	Health Care	Pharmaceuticals
XEL	Xcel Energy	Utilities	Multi-Utilities
EXC	Exelon	Utilities	Electric Utilities
GILD	Gilead Sciences	Health Care	Biotechnology
KHC	Kraft Heinz	Cons Staples	Packaged Foods & Meats
MDLZ	Mondelez International	Cons Staples	Packaged Foods & Meats
PEP	PepsiCo	Cons Staples	Soft Drinks & Beverages

TABLE VII. Level2 Cluster: Health Care/Staples

Ticker	Name	Sector	Sub-Industry
BKR	Baker Hughes	Energy	Oil-Gas Equip/Services
CCEP	Coca-Cola Europacific	Cons Staples	Soft Drinks & Beverages
CHTR	Charter Comms	Comm Services	Cable & Satellite
CMCSA	Comcast	Comm Services	Cable & Satellite
DLTR	Dollar Tree	Cons Staples	Merch Retail
FANG	Diamondback Energy	Energy	Oil-Gas Explo/Production
ROST	Ross Stores	Cons Disc	Apparel Retail
WBD	Warner Bros. Discovery	Comm Services	Broadcasting

TABLE VIII. Level3 Cluster: Staples/Energy

Ticker	Name	Sector	Sub-Industry
ADP	Automatic Data Process	Industrials	HR & Employment Serv
CSCO	Cisco	IT	Communications Equip
CSX	CSX Corporation	Industrials	Rail Transportation
CTAS	Cintas	Industrials	Diversified Support Serv
CTSH	Cognizant	IT	IT Consulting
FAST	Fastenal	Industrials	Trading Comp & Distributors
HON	Honeywell	Industrials	Industrial Conglomerates
KDP	Keurig Dr Pepper	Cons Staples	Soft Drinks & Beverages
LIN	Linde plc	Materials	Industrial Gases
MNST	Monster Beverage	Cons Staples	Soft Drinks & Beverages
ORLY	O'Reilly Automotive	Cons Disc	Automotive Retail
PAYX	Paychex	Industrials	HR & Employment Serv
PCAR	Paccar	Industrials	Const Mach & Transp Equip
ROP	Roper Technologies	IT	Electronic Equip & Instruments
SBUX	Starbucks	Cons Disc	Restaurants
TMUS	T-Mobile US	Comm Serv	Wireless Telecomm Serv
VRSK	Verisk Analytics	Industrials	Research & Consulting Serv

TABLE IX. Level3 Cluster: Industrials

APPENDIX

Consider a graph $G = (V, E, w)$ with vertices V , edges E and weights w , with the degree of vertex v indicated by d_v . We distribute a mass m_x on each of the neighbors of the node x . Now we use the discrete Optimal Transport formulation to define a transport plan, the map $P : V \times V \rightarrow [0, 1]$ such that $P(u, v)$ is the amount of mass at vertex v to be moved to vertex u .

$$\sum_{v' \in V} P(u, v') = m_x(u) \sum_{u' \in V} P(u', v) = m_y(v) \quad (5)$$

the Wasserstein distance $W(m_x, m_y)$ is defined as the minimum total weighted distance to move m_x to m_y

$$W(m_x, m_y) = \min_P \sum_{u, v \in V} d(u, v) P(u, v) \quad (6)$$

The probability distribution m_x for node x must be specified. There are several possibilities to choose this distribution. Here, the probability distribution used for x , m_x^α , with parameter $\alpha \in [0, 1]$, with the set of neigh-

bors of x , $\pi(x)$ is given by

$$m_x^\alpha(x_i) = \begin{cases} \alpha & \text{if } x_i = x \\ \frac{1-\alpha}{d_x} & \text{if } x_i \in \pi(x) \\ 0 & \text{otherwise} \end{cases} \quad (7)$$

Here d_x is the normalization factor given by the degree of x and α measures the probability to remain at x . In practice, it corresponds to distributing a unit mass over the site x and all its nearest neighbors, with α on x and $1 - \alpha$ uniformly divided among the neighbors of x . This can be interpreted as a lazy random walk with α representing the probability of remaining at the site x . In the literature, α is known as the idleness parameter, with $\alpha = 0$ representing the random walk and $\alpha = 1$ the fully idle case. We define the α -Ricci curvature, κ_{xy}^α as

$$\kappa_{xy}^\alpha = 1 - \frac{W(m_x^\alpha, m_y^\alpha)}{d(x, y)} \quad (8)$$

For $\alpha = 1$, we see that the curvature $\kappa_{xy} = 0$. Lin-Lu-Yau[12] introduced a new limiting Ollivier-Ricci curvature, $\bar{\kappa}$

$$\bar{\kappa} = \lim_{\alpha \rightarrow 1} \frac{\kappa_{ij}}{1 - \alpha} \quad (9)$$

They showed that the limit $\alpha \rightarrow 1$, of this quantity exists. In this paper, we use the value of $\alpha = 1/2$, as widely used in the literature[27] and refer to the α -Ricci curvature as the Ricci curvature.